Intercalation of Cyclic Ethers into Vanadyl Phosphate

Vítězslav Zima,*[a] Klára Melánová,[a] Ludvík Beneš,[a] Pavla Čapková,[b] Miroslava Trchová,[b] and Pavel Matějka[c]

Abstract: Two cyclic ethers, tetrahydrofuran (THF) and tetrahydropyran (THP), were intercalated into vanadyl phosphate and characterized by X-ray powder diffraction, thermogravimetry, and IR and Raman spectroscopy. Both compounds contain one molecule of ether per formula unit of $VOPO_4$ and show high thermal stability in comparison with $VOPO_4$ intercalates with other organic guest molecules. Both ethers are anchored to the $VOPO_4$ host layers by their oxygen atoms, which are coordinated to the vanadium atoms of the host. The probable arrangement of the tetrahydropyran molecules in the host interlayer space is derived from molecular simulations by the Cerius^2 4.5 program.

Keywords: intercalations · molecular modeling · vanadium · vibrational spectroscopy · X-ray diffraction

Introduction

Vanadyl phosphate dihydrate $VOPO_4 \cdot 2H_2O$ and other isostructural layered compounds are able to accommodate some types of organic molecules in the interlayer space.[1] Aliphatic alcohols[2–5] and diols,[2, 6] amines,[7, 8] carboxylic acids,[9] carboxamides,[10] amino acids,[11] ketones,[12] and aldehydes[13] are amongst the compounds, which can be intercalated in such a way. A great deal of attention was devoted to the intercalation of heterocyclic N and S donors. Pyridine and its derivatives,[14] imidazole,[15] pyrazole, pyrazine, and phenazine,[16] pyrrole and their derivatives,[17, 18] 2,2′-dithiodipyridine,[19] and tetrathiofulvalene[20] were also intercalated into vanadyl phosphate. On the other hand, intercalation of heterocycles with O donors into vanadyl phosphate has not been described yet. Intercalations of some crown ethers into montmorillonite[21, 22] and vanadium oxide xerogel[23] were studied. In these materials, some of the water molecules in their interlayer space are replaced by crown ethers. Recently, poly(ethylene glycol)s were intercalated into vanadyl phosphate and isostructural niobyl phosphate and arsenate.[24] It is presumed that the chains of the guests are deposited parallel to the host layer with every other oxygen atom of the guest coordinated to the vanadium or niobium atoms of the host layer. The chains are arranged in a bimolecular way in the interlayer space. Two types of $VOPO_4$ intercalates were formed depending on the temperature of the reaction. The high-temperature phase contains half the amount of the guest, and the guest chains are arranged in a monomolecular way.

The present paper reports the results of the intercalation of tetrahydrofuran (THF) and tetrahydropyran (THP) into vanadyl phosphate.

[a] Dr. V. Zima, Dr. K. Melánová, Dr. L. Beneš
Joint Laboratory of Solid State Chemistry
University of Pardubice, Studentská 84
53210 Pardubice (Czech Republic)
Fax: (+420) 40-603-6011
E-mail: vitezslav.zima@upce.cz

[b] Dr. P. Čapková, Dr. M. Trchová
Faculty of Mathematics and Physics
Charles University, V Holešovičkách 2
18000 Praha (Czech Republic)

[c] Dr. P. Matějka
Department of Analytical Chemistry
Institute of Chemical Technology, Technická 5
16628 Praha (Czech Republic)

Results and Discussion

Both guests cannot be intercalated directly in anhydrous vanadyl phosphate, and replacement of water molecules in $VOPO_4 \cdot 2H_2O$ does not lead to an intercalation. The intercalates had to be prepared by replacing 1-propanol or 2-propanol in the corresponding $VOPO_4$ intercalate with the desired guest. The intercalates prepared were yellow crystalline solids, and this indicates that the vanadium(v) had not been significantly reduced. As confirmed by the results of elemental analyses, both intercalates contain one molecule of guest per formula unit.

The diffractograms of both intercalates show a series of sharp (00*l*) reflections (Figure 1). The diffractogram of the THF intercalate contains a number of (*hkl*) diffraction lines that provide evidence of a regular structure. The lattice

  0947-6539/02/0807-1703 $ 20.00+.50/0

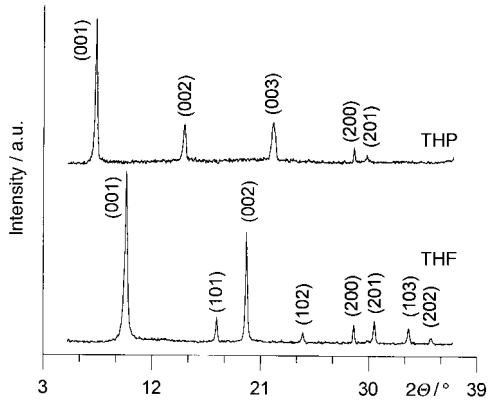

Figure 1. X-ray powder diffractograms of $VOPO_4 \cdot THF$ and $VOPO_4 \cdot THP$.

parameters of the tetragonal structure are $a = 6.207(2)$ Å and $c = 8.932(3)$ Å for the THF intercalate and $a = 6.201(2)$ Å and $c = 12.014(2)$ Å for the THP intercalate.

Both intercalates are more stable in air (at relative humidity about 40%) than 1-alkanol,[2] 1,2-alkanediol,[25] or acetone[12] intercalates. The diffraction line (001) of vanadium phosphate dihydrate was not observed after more than seven days, whereas this line appeared after one hour for acetone-intercalated $VOPO_4$.

A surprisingly high thermal stability was found for the $VOPO_4$ intercalate with THF. The position and the intensity of the diffraction lines did not change up to 160 °C. Above this temperature, the intensity of the diffraction lines decreases, and THF is released slowly as confirmed by the thermogravimetric results. The total weight loss (31%) corresponds to the formula $VOPO_4 \cdot C_4H_8O$. Visible reflectance spectra of the freshly prepared THF intercalate (1) and after heating at 160 °C (2) together with spectra of $VOPO_4 \cdot 2H_2O$ and $Na_{0.015}VOPO_4 \cdot 2H_2O$ containing 1.5% vanadium(IV) are given in Figure 2. Both spectra of the intercalate are similar to that of $VOPO_4 \cdot 2H_2O$, which indicates that vanadium(V) is not significantly reduced during the heating. The high thermal

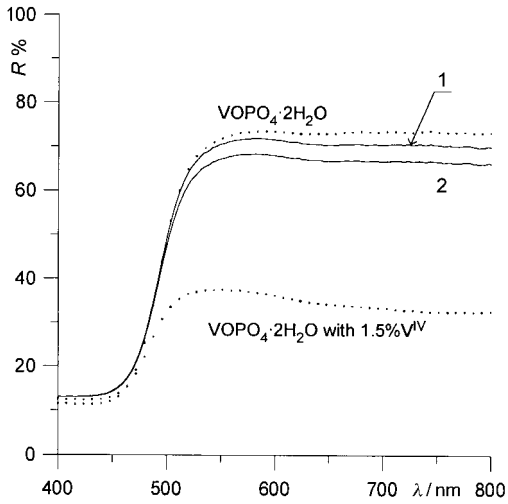

Figure 2. Visible reflection spectra of $VOPO_4 \cdot 2H_2O$, $Na_{0.015}VOPO_4 \cdot 2H_2O$, and the $VOPO_4 \cdot THF$ intercalate before (1) and after heating to 160 °C (2).

stability of the THF intercalate indicates a very strong interaction between the guest species and the host layers.

Interesting thermal behavior of the THP intercalate was observed. The dependence of the basal spacing of the intercalate on temperature is shown in Figure 3. The basal spacing slightly increases up to 85 °C. At this temperature, a new phase with the basal spacing 12.8 Å appears. Another

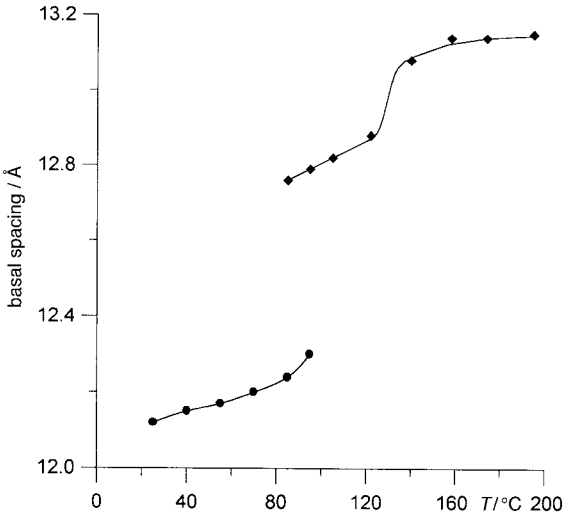

Figure 3. Basal spacings of $VOPO_4 \cdot THP$ as a function of temperature.

weak increase of the basal spacing up to 122 °C is followed by a significant increase of the basal spacing (13.14 Å at 158 °C), which is accompanied by a broadening of the (00*l*) diffraction lines. Both steps are reversible during cooling. At higher temperatures, the intensity of the (00*l*) diffraction lines decreases due to slow decomposition of the intercalate. The *a* parameter of the tetragonal lattice does not change up to 158 °C. The color of the intercalate does not change up to 122 °C and then it turns yellow-green. This indicates a gradual reduction of vanadium(V).

The THP intercalate is also very stable. Its thermal decomposition starts at 140 °C, and THP is slowly released up to 600 °C, as confirmed by the TG measurements (Figure 4). The total weight loss of 33.8% corresponds to the formula $VOPO_4 \cdot C_5H_{10}O$ (calculated 34.7%). There are two endothermic effects on the DTA curve that occur at the temperatures 78 and 126 °C when the step changes of the basal spacing are observed. No weight loss accompanies these effects (Figure 4). The exothermic effects at higher temperatures are probably due to the combustion of the released compounds.

FTIR and Raman spectroscopy: The infrared spectra of liquid THP and its intercalate in $VOPO_4$ in the region from 1500 to 650 cm^{-1} and the Raman spectra are shown in Figures 5 and 6. The intense band at 944 cm^{-1} in the Raman spectrum of the intercalate corresponds most probably to the symmetric $\nu(PO_4)$ stretching vibration of tetrahedral phosphorus in $(VOPO_4)_\infty$. The sharp band at 995 cm^{-1} came from the V=O vanadyl stretching vibration. With the help of the Raman spectrum, we can assign the band at 974 cm^{-1} in the infrared

  0947-6539/02/0807-1704 $ 20.00+.50/0 *Chem. Eur. J.* **2002**, *8*, No. 7

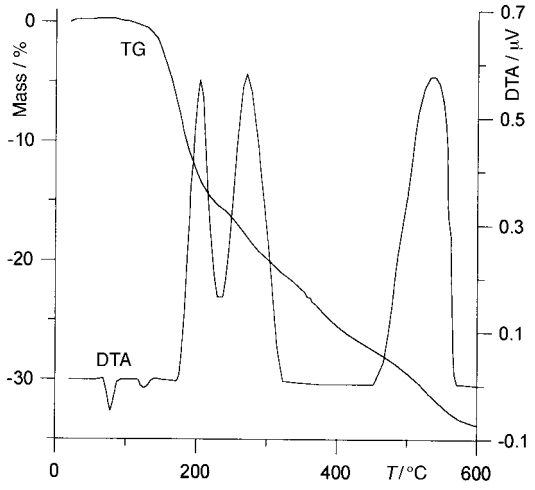

Figure 4. TG-DTA of $VOPO_4 \cdot THP$.

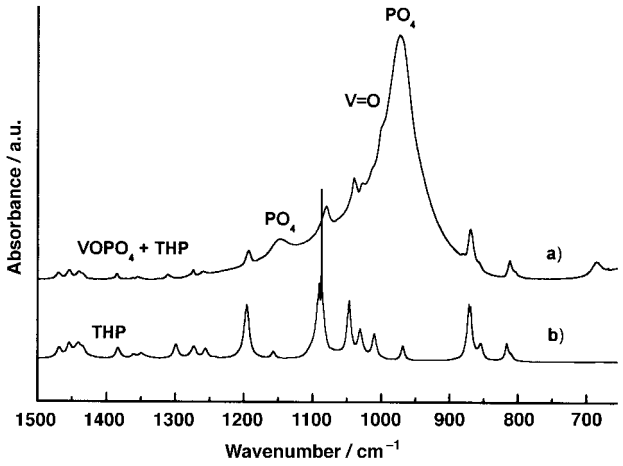

Figure 5. FTIR spectra of $VOPO_4 \cdot THP$ (in KBr pellet) (a) and liquid THP (ATR on ZnSe crystal) (b) in the region from 1500 to 650 cm^{-1}.

spectrum to the symmetric $\nu(PO_4)$ stretching vibration, which is infrared active due to the distortion of the tetrahedral phosphorus of the intercalate. The shoulder at 1000 cm^{-1} in the infrared spectrum is most probably the V=O stretching band of the vanadyl group. Its position corresponds to the

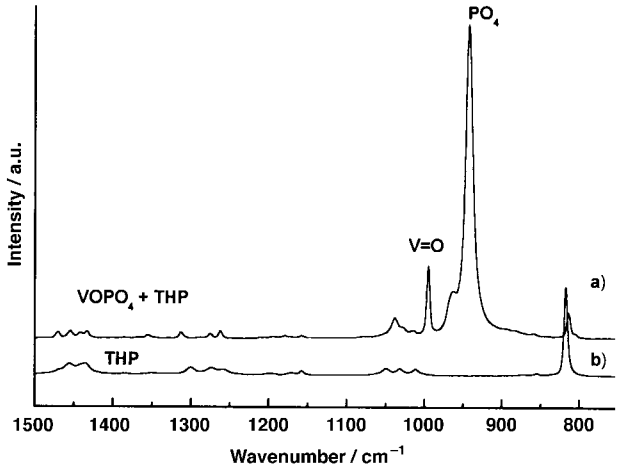

Figure 6. Raman spectra of $VOPO_4 \cdot THP$ (a) and liquid THP (b) in the region from 1500 to 750 cm^{-1}.

coordination of the oxygen atom of THP in the vanadyl octahedron. The vanadyl stretching band appears to be especially sensitive to atoms coordinated to vanadium within the octahedral arrangement. Intercalation of water molecules into anhydrous $VOPO_4$ shifts the V=O band from 1035 to 995 cm^{-1} typical for mono- and dihydrates.[26] The band of the stretching V=O vibration is observed at the same position (995 cm^{-1}) in the spectra of $VOPO_4 \cdot 2C_2H_5OH$ and $VOPO_4 \cdot 2H_2O$.[27] This indicates that both guest molecules are anchored to the host layers by similar bonds, and therefore no large change in the bond energy is expected during the reaction. Intercalation of acetone led to a shoulder at 1002 cm^{-1} for the band of the V=O stretching vibration in the infrared spectrum.[28] For 5-hexyn-1-ol intercalated in $VOPO_4$, this shoulder was observed at 1007 cm^{-1}.[3]

The band at 1148 cm^{-1} in the infrared spectrum of the intercalate with THP is the asymmetric $\nu(PO_4)$ stretching vibration of the phosphorous tetrahedron. The position of the main spectral bands of the host structure only slightly differs from those of anhydrous vanadyl phosphate or its hydrated form.[26] It confirms that the structure of the original $VOPO_4$ layers remains unchanged after the intercalation reaction.

The infrared and Raman spectra of the THP intercalate[29, 30] differ in the 3100–2700 cm^{-1} region in terms of the position, shape, and intensity of the corresponding bands of liquid THP. Due to the fixation of the intercalated molecules in the interlayer space, the asymmetric CH_2 stretching bands at 2960 and 2852 cm^{-1} split into several bands, and a new doublet shifted to 3006 and 2997 cm^{-1} appears in the Raman spectrum of the intercalated THP (Figure 7). The

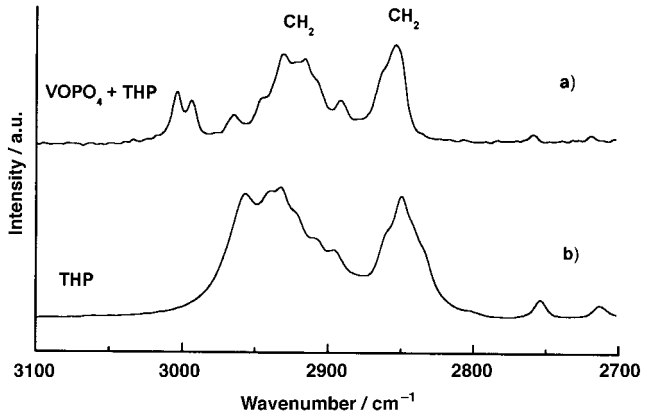

Figure 7. Raman spectra of $VOPO_4 \cdot THP$ (a) and liquid THP (b) in the region from 3100 to 2700 cm^{-1}.

new band with the maximum at 2994 cm^{-1} and a shoulder at about 3000 cm^{-1} is observed in the infrared spectrum (Figure 8). Intercalation changes the scissoring (several bands from 1380 to 1470 cm^{-1}), wagging (at about 1350 cm^{-1}), twisting (at about 1250 cm^{-1}), and rocking (at about 1150 cm^{-1}) vibrations of the CH_2 groups.[29, 30] The band of the asymmetric (at about 1088 cm^{-1}) C–O–C ring vibration is overlapped by the PO_4 vibrations of vanadyl phosphate. The position of the deformation ring vibration is shifted from 818 to 815 cm^{-1} in the Raman spectrum (Figure 6) and from 816 to 812 cm^{-1} in the infrared spectrum (Figure 5). The peak of the

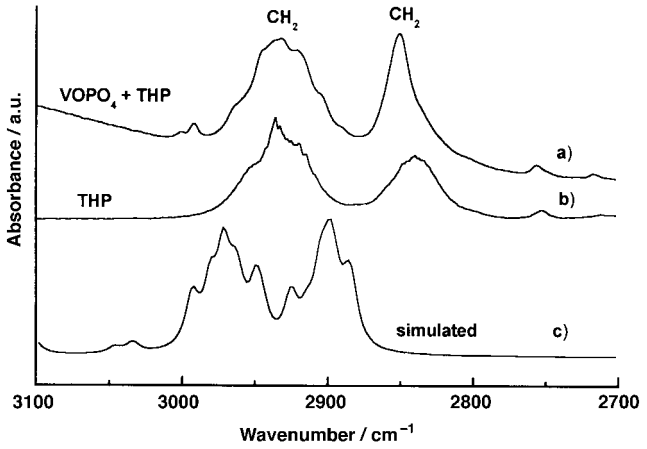

Figure 8. FTIR spectra of $VOPO_4 \cdot THP$ (in KBr pellet) (a), liquid THP (ATR on ZnSe crystal) (b), and the simulated IR spectrum of $VOPO_4 \cdot THP$ (c) in the region from 3100 to 2700 cm^{-1}.

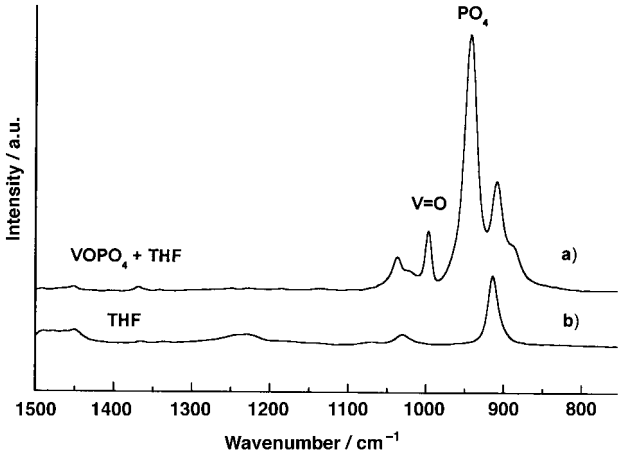

Figure 10. Raman spectra of $VOPO_4 \cdot THF$ (a) and liquid THF (b) in the region from 1500 to 750 cm^{-1}.

deformation ring vibration at 872 cm^{-1} in the infrared spectrum of THP is shifted to 869 cm^{-1} (Figure 5).

The infrared and Raman spectra of liquid THF and its $VOPO_4$ intercalate in the region from 1500 to 650 cm^{-1} are given in Figures 9 and 10. The Raman band of the symmetric $\nu(PO_4)$ stretching vibration of the phosphorous tetrahedron is situated at 944 cm^{-1}. The sharp band at 1001 cm^{-1} corresponds to the V=O vanadyl stretching vibration. This allowed us to distinguish these bands from other bands belonging to the intercalated THF molecules in the infrared spectrum of the intercalate. The band of the symmetric $\nu(PO_4)$ stretching vibration has a maximum at about 963 cm^{-1} in the infrared spectrum, and the vanadyl stretching vibration is observed as a shoulder at 1004 cm^{-1}. The smaller value of the shift of the vanadyl stretching vibration of the THF intercalate in the Raman spectrum is caused by the fact that THF forms a monolayer in the interlayer space with a higher density of guest molecules compared with THP.

The mutual interaction of the THF molecules in the intercalate leads to the splitting of the bands in the region 1500 – 650 cm^{-1}. The fundamental bending vibrations of CH_2 occur in the infrared spectrum in this region: scissoring at about 1458 cm^{-1}, wagging at about 1364 cm^{-1}, and twisting at about 1182 cm^{-1}. The biggest change between liquid and intercalated THF is shown by the asymmetric vibrations of the C–O–C ring. In the infrared spectrum of THF, this intensity is very strong at 1061 with a shoulder at 1031 cm^{-1}, and the corresponding maximum is shifted from 1061 in the liquid state to 1039 cm^{-1} in the intercalate. Similarly, the band of the symmetric vibrations of the C–O–C ring at 918 cm^{-1} for liquid THF is observed at 918 cm^{-1} with a shoulder at 914 cm^{-1} in the Raman spectrum of the intercalate. In the infrared spectrum, this band is observed at 914 cm^{-1} and is split into several bands between 921 and 891 cm^{-1} for the intercalate. This can be explained by the two different positions of the THF molecules in the intercalate.[31]

The positions of the bands of the asymmetric stretching vibrations of CH_2 are shifted from 2964 and 2873 cm^{-1} to higher values (2982 and 2891 cm^{-1}) in the Raman spectrum going from the liquid state to the intercalate. This shift is more pronounced than in the case of THP, but no new bands above 3000 cm^{-1} were observed in the Raman and infrared spectra (Figures 11 and 12) as was observed in the case of THP.

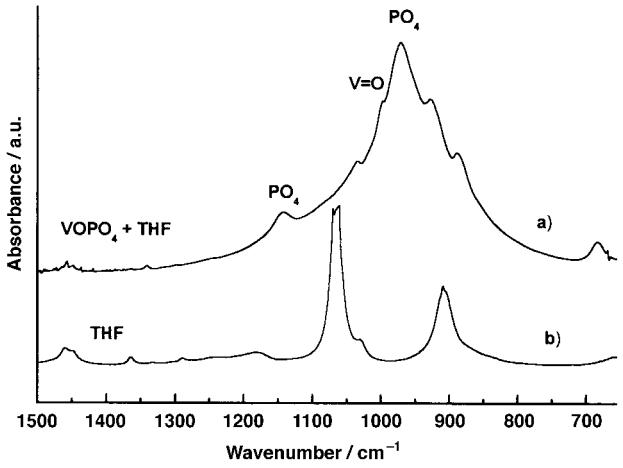

Figure 9. FTIR spectra of $VOPO_4 \cdot THF$ (in KBr pellet) (a) and liquid THF (ATR on ZnSe crystal) (b) in the region from 1500 to 650 cm^{-1}.

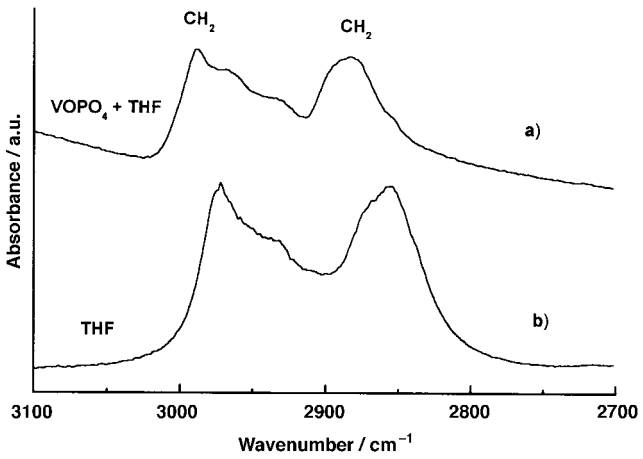

Figure 11. FTIR spectra of $VOPO_4 \cdot THF$ (in KBr pellet) (a) and liquid THF (ATR on ZnSe crystal) (b) in the region from 3100 to 2700 cm^{-1}.

0947-6539/02/0807-1706 $ 20.00+.50/0 *Chem. Eur. J.* **2002**, *8*, No. 7

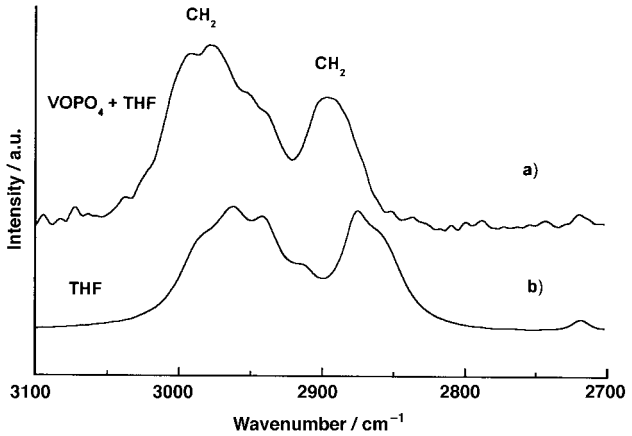

Figure 12. Raman spectra of $VOPO_4 \cdot THF$ (a) and liquid THF (b) in the region from 3100 to 2700 cm^{-1}.

Molecular simulations of $VOPO_4 \cdot THP$: $VOPO_4$ intercalated with tetrahydrofuran (THF) shows a diffraction pattern with good resolution that allowed us to determine the crystal structure.[31] The diffractogram of $VOPO_4$ intercalated with tetrahydropyran (THP) reveals the structural disorder due to the mutual shifts of the two successive host layers. For $VOPO_4 \cdot THP$, we can observe only (00*l*) reflections with two weak (200) and (201) reflections at about $2\Theta = 30^\circ$ (Figure 1). In such a case, the structure model, including the characterization of the disorder, can be obtained by using empirical force field.

Molecular mechanics and molecular dynamics simulations of $VOPO_4 \cdot THP$ were carried out in the Cerius^2 4.5 modeling environment. The strategy of the modeling was based on the generally accepted assumption of rigid $VOPO_4$ layers.[28, 32] This assumption was confirmed by comparing the structure of the $VOPO_4$ layers before and after intercalation of THF.[31, 33] The initial model of $VOPO_4 \cdot THP$ was based on the tetragonal unit cell of the host structure, and the *c* parameter was extended to the basal spacing of 12.0 Å. The THP molecules in a chairlike conformation were inserted into the interlayer space and attached to the vanadium atoms through its O_{THP} oxygen atoms. The $V{-}O_{THP}$ distance was set up to 2.41 Å. This value was taken from the diffraction data for the THF intercalate[31] and fixed during the energy minimization, as the force fields available in the Cerius^2 4.5 library cannot describe properly the $V{-}O_{THP}$ interaction.

The energy minimization was carried out in a Minimizer module in Cerius^2 4.5 by using Universal force field[34] under the following constraints: rigid but movable host layers, fixed $V{-}O_{THP}$ distance, and variable positions of all atoms in the THP guest molecules, with the exception of O_{THP}. Cell parameters *a*, *b*, and γ were kept fixed, and *c*, α, and β were variable during energy minimization. Molecular dynamics simulations were carried out to check the conformational behavior of the THP molecules in the interlayer space of $VOPO_4$. Quenched dynamics calculations in the NVT (constant–volume/constant–temperature dynamics) ensemble were performed at 300 K with time steps of 0.001 ps. Results of the dynamics simulations confirmed the chairlike conformation of the THP molecules in the interlayer space of $VOPO_4$ at room temperature.

Molecular simulations showed the bilayer arrangement of the THP molecules in the interlayer space, in which the guest layers are slightly overlapping (Figure 13). Figure 14 illustrates the anchoring of the THP molecules to the $VOPO_4$ layers by $V{-}O_{THP}$ bonds. The O_{THP} oxygen atom completes the octahedral coordination of the vanadium atoms. According to the molecular simulations, there are two possible orientations of the THP molecules. The THP ring can be oriented with the same probability in two different ways with respect to the $VOPO_4$ layer (Figure 15a and b). These two THP orientations making the angle 90° between the THP rings are the consequence of the tetragonal symmetry of the $VOPO_4$ layer. The two arrangements of the THP molecules in Figure 15a,b exhibit the same crystal energy. The basal spacing of 12.3 Å obtained from modeling is in good agreement with the experimental value of 12.0 Å.

Figure 15a,b also illustrates the type and degree of disorder. For clarity, only the THP molecules are visualized in the unit cell. One sees the mutual shift of the successive $VOPO_4$ layers. The values of the shift vectors were found between ≈ 0.3–0.6 Å, predominantly in the *100* direction. This disorder in the layer stacking leads to a diffraction pattern, in which most of the nonbasal reflections are smoothed or missing, and the basal reflections are dominant. In addition, the influence of this effect increases by the preferred orientation of the crystallites.

The molecular simulations also helped us to elucidate the positions and profiles of the IR and Raman spectra and led to the following conclusions. In both cases of pristine THF and THP, the IR and Raman spectra exhibit two bands corre-

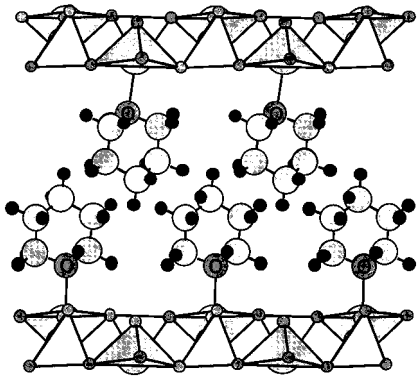

Figure 13. Side view of the structure $VOPO_4 \cdot THP$.

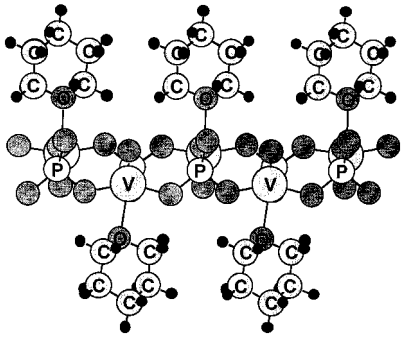

Figure 14. Anchoring of the THP molecules to the $VOPO_4$ layers.

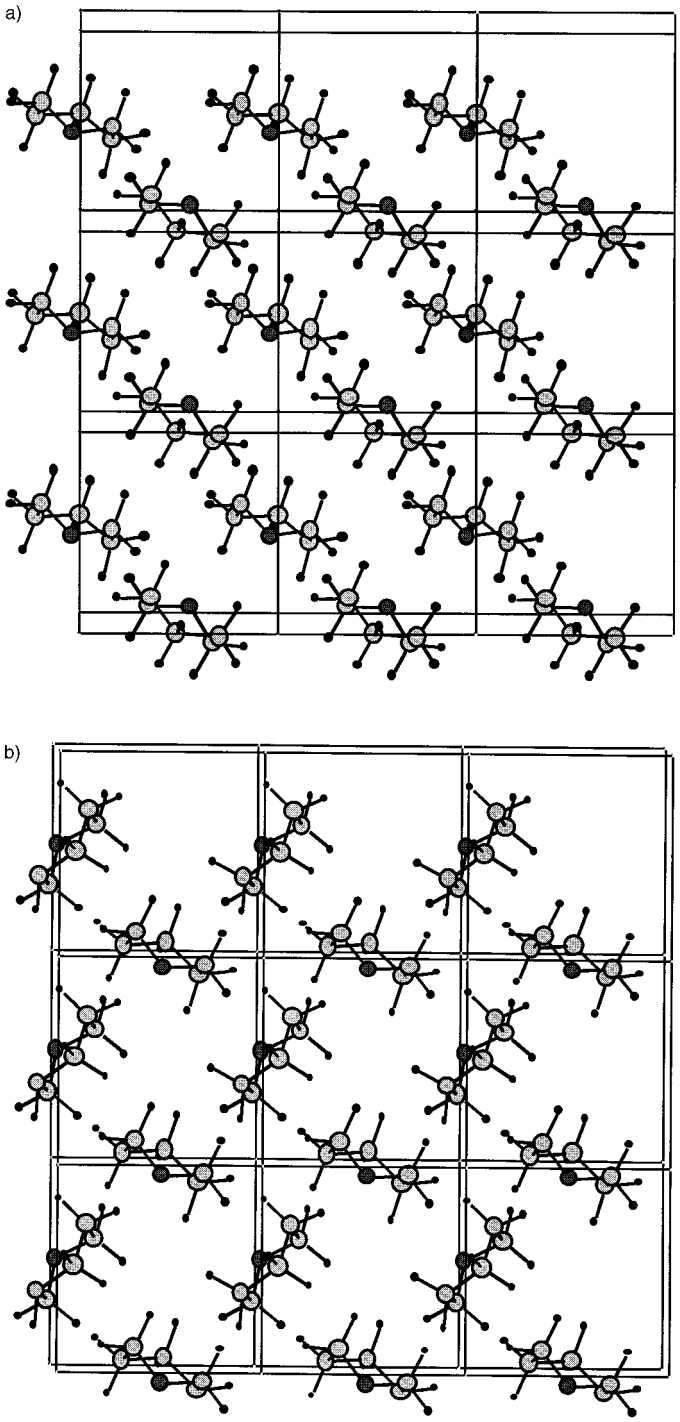

Figure 15. Two arrangements of the THP molecules in the interlayer space of $VOPO_4$: (a) parallel and (b) perpendicular orientation of THP rings in the upper and lower layer in the interlayer space. Both arrangements exhibit the same crystal energy.

sponding to CH_2 stretching vibrations between ≈2800 and 3000 cm^{-1} (Figures 7, 8, 11, and 12). The first band at about 2850 cm^{-1} corresponds to the symmetric CH_2 stretching vibration, and the second more broadened band in the region of 2900 – 3000 cm^{-1} corresponds to the asymmetric CH_2 stretching vibration. Comparing the spectra of pristine THP and THF with the spectra of $VOPO_4 \cdot$THP and $VOPO_4 \cdot$THF, one sees the shift of these CH_2 stretching bands to the higher wavenumbers. This shift is stronger for $VOPO_4 \cdot$THF than for $VOPO_4 \cdot$THP. This is a consequence of the different arrangement of these molecules in the interlayer space. While the THF molecules are arranged in a monolayer,[31] THP molecules in a bilayer arrangement are not so densely packed (Figure 13).

In the case of $VOPO_4 \cdot$THP, the band corresponding to the asymmetric CH_2 stretching vibration in the IR and Raman spectra exhibits a large amount of splitting and broadening. As a consequence of this large amount of splitting, we observe a new small side double band at about 3000 cm^{-1}. Simulation of the IR and Raman spectra revealed that this new band corresponds also to the asymmetric CH_2 stretching vibrations. The simulated IR spectrum for $VOPO_4 \cdot$THP in the region 2700 – 3000 cm^{-1} is shown in Figure 8 as curve c. A small difference between the calculated and experimental values is given by an approximation of the bond situations in empirical force field calculations.

The simulated spectrum is in good agreement with the experimental one with respect to the character of the spectrum and the positions of the bands. This is also an indication that the structure model of $VOPO_4 \cdot$THP obtained from the molecular simulations is in good agreement with the experimental data.

Experimental Section

Preparation: Vanadyl phosphate dihydrate was prepared by prolonged boiling of a mixture of vanadium pentoxide and phosphoric acid in water.[35] The product was filtered and washed with distilled water several times.

The propanol intercalate was prepared by suspending microcrystalline $VOPO_4 \cdot 2H_2O$ in dry propanol and subsequent short exposure to a microwave field.[2] The intercalation compounds were obtained by displacing propanol in $VOPO_4 \cdot 2C_3H_7OH$ by THF or THP. The propanol intercalate (1 g) was dispersed in THF or THP (50 mL) and stirred for one day at room temperature. The intercalates were filtered off and dried in nitrogen.

The composition of the intercalates was determined by elemental analysis (C, H). elemental analysis calcd (%) for $VOPO_4 \cdot C_4H_8O$: C 20.53, H 3.45; found: C 20.61, H 3.39; elemental analysis calcd (%) for $VOPO_4 \cdot C_5H_{10}O$: C 24.21, H 4.06; found: C 24.53, H 4.11.

XRD: Powder data were obtained with an X-ray diffractometer HZG-4 (Freiberger Präzisionsmechanik, Germany) by using $Cu_{K\alpha}$ radiation with discrimination of the $Cu_{K\beta}$ radiation by a Ni filter. Diffraction angles were measured from 5 to 50° (2θ). The temperature measurements from 20 to 250 °C were carried out on a heated corundum plate with a thermocouple.[36]

Thermogravimetry: The TG analyses were performed by using a Derivatograph C (MOM Budapest, Hungary). The measurements were carried out in air between 20 and 500 °C at a heating rate of 5 K min^{-1}.

UV/Vis spectroscopy: UV/Vis diffuse reflectance spectra were measured on a dual-beam UV/Vis-NIR spectrometer JASCO V570 equipped with an integrating sphere attachment ISN-470.

Infrared measurements: Infrared measurements in the range 400 – 4000 cm^{-1} were made with a fully computerized Nicolet IMPACT 400 FTIR spectrometer (300 scans per spectrum at 2 cm^{-1} resolution). Measurements of the intercalates were performed ex situ in the transmission mode in KBr pellets. The spectra of the corresponding liquid ethers were measured by the baseline horizontal attenuated total reflection (ATR) technique on a ZnSe crystal. The spectra were corrected for the content of H_2O and CO_2 in the optical path.

Raman spectral measurements: FT Raman spectra were collected by using a Fourier transform near-infrared (FT-NIR) spectrometer Equinox 55/S

0947-6539/02/0807-1708 $ 20.00+.50/0 *Chem. Eur. J.* **2002**, *8*, No. 7

(Bruker) equipped with FT Raman module FRA 106/S (Bruker) (128 interferograms were co-added per spectrum in the range 4000 – 700 cm^{-1} at 4 cm^{-1} resolution).

Acknowledgements

This study was supported by the Grant Agency of the Czech Republic (Grant No. 202/01/0520).

[1] J. Kalousová, J. Votinský, L. Beneš, K. Melánová, V. Zima, *Collect. Czech. Chem. Commun.* **1998**, *63*, 1 – 19.
[2] L. Beneš, K. Melánová, V. Zima, J. Kalousová, J. Votinský, *Inorg. Chem.* **1997**, *36*, 2850 – 2854.
[3] L. Beneš, K. Melánová, V. Zima, M. Trchová, E. Uhlířová, P. Matějka, *Eur. J. Inorg. Chem.* **2001**, 713 – 719.
[4] L. Beneš, K. Melánová, V. Zima, *Eur. J. Inorg. Chem.* **2001**, 1883 – 1887.
[5] L. Beneš, V. Zima, K. Melánová, *J. Inclusion Phenom.* **2001**, *40*, 131 – 138.
[6] L. Beneš, K. Melánová, V. Zima, *J. Solid State Chem.* **2000**, *151*, 225 – 230.
[7] K. Beneke, G. Lagaly, *Inorg. Chem.* **1983**, *22*, 1503 – 1507.
[8] L. Beneš, R. Hyklová, J. Kalousová, J. Votinský, *Inorg. Chim. Acta* **1990**, *177*, 71 – 74.
[9] L. Beneš, J. Votinský, J. Kalousová, K. Handlíř, *Inorg. Chim. Acta* **1990**, *176*, 255 – 259.
[10] M. Martinez-Lara, L. Moreno-Real, A. Jimenez-Lopez, S. Bruque-Gamez, A. Rodriguez-Garcia, *Mater. Res. Bull.* **1986**, *21*, 13 – 23.
[11] V. Zima, L. Beneš, K. Melánová, *Solid State Ionics* **1998**, *106*, 285 – 290.
[12] K. Melánová, L. Beneš, V. Zima, P. Čapková, M. Trchová, *Collect. Czech. Chem. Commun.* **1999**, *64*, 1975 – 1979.
[13] K. Melánová, L. Beneš, V. Zima, *J. Solid State Chem.* **2001**, *157*, 50 – 55.
[14] J. W. Johnson, A. J. Jacobson, J. F. Brody, S. M. Rich, *Inorg. Chem.* **1982**, *21*, 3820 – 3825.
[15] A. De Stefanis, A. A. G. Tomlinson, *J. Mater. Chem.* **1994**, *5*, 319 – 322.
[16] A. De Stefanis, S. Foglia, A. A. G. Tomlinson, *J. Mater. Chem.* **1995**, *5*, 475 – 483.
[17] G. Matsubayashi, H. Nakajima, *Chem. Lett.* **1993**, 31 – 34.
[18] H. Nakajima, G. Matsubayashi, *J. Mater. Chem.* **1994**, *4*, 1325 – 1329.
[19] T. Yatabe, G. Matsubayashi, *J. Mater. Chem.* **1996**, *6*, 1849 – 1852.
[20] R. Pozas-Tormo, L. Moreno-Real, S. Bruque-Gamez, M. Martinez-Lara, J. Ramos-Barado, *Mater. Sci. Forum* **1992**, *91 – 93*, 511 – 516.
[21] P. Aranda, E. Ruiz-Hitzky, *Acta Polym.* **1994**, *45*, 59 – 67.
[22] P. Aranda, J. C. Galvan, B. Casal, E. Ruiz-Hitzky, *Colloid Polym. Sci.* **1994**, *272*, 712 – 720.
[23] E. Ruiz-Hitzky, P. Aranda, B. Casal, *J. Mater. Chem.* **1992**, *2*, 581 – 582.
[24] K. Melánová, L. Beneš, V. Zima, R. Vahalová, M. Kilián, *Chem. Mater.* **1999**, *11*, 2173 – 2178.
[25] K. Melánová, L. Beneš, V. Zima, *J. Inclusion Phenom.* **2000**, *36*, 301 – 309.
[26] M. Trchová, P. Čapková, P. Matějka, K. Melánová, L. Beneš, *J. Solid State Chem.* **1999**, *148*, 197 – 204.
[27] L. Beneš, K. Melánová, M. Trchová, P. Čapková, P. Matějka, *Eur. J. Inorg. Chem.* **1999**, 2289 – 2294.
[28] P. Čapková, M. Trchová, V. Zima, H. Schenk, *J. Solid State Chem.* **2000**, *150*, 356 – 362.
[29] N. Bagget, S. A. Barker, A. B. Foster, R. H. Moore, D. H. Whiffen, *J. Am. Chem. Soc.* **1960**, *82*, 4565 – 4570.
[30] J. M. Eyster, E. W. Prohofsky, *Spectrochim. Acta* **1974**, *30A*, 2041 – 2046.
[31] K. Goubitz, P. Čapková, K. Melánová, W. Molleman, H. Schenk, *Acta Crystallogr.* **2001**, *B57*, 178 – 183.
[32] P. Čapková, D. Janeba, L. Beneš, K. Melánová, H. Schenk, *J. Mol. Model.* **1998**, *4*, 150 – 157.
[33] M. Tachez, F. Theobald, J. Bernard, A. W. Hewat, *Rev. Chim. Miner.* **1982**, *19*, 291 – 300.
[34] K. Rappe, C. J. Casewit, K. S. Colwell, W. A. Goddard, W. M. Skiff, *J. Am. Chem. Soc.* **1992**, *114*, 10024—10035.
[35] G. Ladwig, *Z. Anorg. Allg. Chem.* **1965**, *338*, 266 – 278.
[36] L. Beneš, *Sci. Pap. Univ. Pardubice Ser. A* **1996**, *2*, 151 – 155.

Received: August 3, 2001 [F3466]

  0947-6539/02/0807-1709 $ 20.00+.50/0